THE JOURNAL OF BIOLOGICAL CHEMISTRY VOL. 286, NO. 6, pp. 4248–4256, February 11, 2011

Iron Promotes the Toxicity of Amyloid β Peptide by Impeding Its Ordered Aggregation*[S]

Received for publication, June 29, 2010, and in revised form, December 1, 2010 Published, JBC Papers in Press, December 8, 2010, DOI 10.1074/jbc.M110.158980

Beinan Liu[‡§], Aileen Moloney[‡§], Sarah Meehan[¶1], Kyle Morris[‖], Sally E. Thomas[‡], Louise C. Serpell[‖], Robert Hider[**], Stefan J. Marciniak[‡], David A. Lomas[‡], and Damian C. Crowther[‡§2]

From the [‡]Department of Medicine, Cambridge Institute for Medical Research, University of Cambridge, Wellcome Trust/Medical Research Council Building, Hills Road, Cambridge CB2 0XY, the [§]Department of Genetics, University of Cambridge, Downing Street, Cambridge CB2 3EH, the [¶]Department of Chemistry, University of Cambridge, Lensfield Road, Cambridge CB2 1EW, the [‖]Department of Biochemistry, School of Life Sciences, University of Sussex, Falmer, Sussex BN1 6PD, and the [**]Department of Chemical Biology, Pharmaceutical Science Research Division, King's College London, London WC2R 2LS, United Kingdom

We have previously shown that overexpressing subunits of the iron-binding protein ferritin can rescue the toxicity of the amyloid β (Aβ) peptide in our *Drosophila* model system. These data point to an important pathogenic role for iron in Alzheimer disease. In this study, we have used an iron-selective chelating compound and RNAi-mediated knockdown of endogenous ferritin to further manipulate iron in the brain. We confirm that chelation of iron protects the fly from the harmful effects of Aβ. To understand the pathogenic mechanisms, we have used biophysical techniques to see how iron affects Aβ aggregation. We find that iron slows the progression of the Aβ peptide from an unstructured conformation to the ordered cross-β fibrils that are characteristic of amyloid. Finally, using mammalian cell culture systems, we have shown that iron specifically enhances Aβ toxicity but only if the metal is present throughout the aggregation process. These data support the hypothesis that iron delays the formation of well ordered aggregates of Aβ and so promotes its toxicity in Alzheimer disease.

AD[3] remains the most common cause of dementia in the elderly; however, our incomplete understanding of its pathogenesis hinders therapeutic progress. It is widely believed that an important initiating factor is the accumulation of the amyloid β peptide (Aβ) within the brain (1, 2). Aβ is generated by the proteolytic processing of the amyloid precursor protein, and the behaviors of the resulting peptide isoforms, largely $Aβ_{1-40}$ and $Aβ_{1-42}$, are determined in large part by differences in their C-terminal residues. In the case of $Aβ_{1-40}$, the peptide is 40 amino acids long and does not contain the final two hydrophobic residues that are present in the more aggregation-prone $Aβ_{1-42}$. In some families, mutations in the *APP* gene result in amino acid substitutions within the Aβ peptide; a particular example of this is the Arctic mutation (E22G) that is linked to early onset autosomal dominant AD (3). In both sporadic and familial AD, however, it is the aggregation-prone Aβ peptide that comprises the amyloid plaques that are seen in the brain of individuals with AD (4). However, the mature amyloid fibrils that constitute these plaques are not thought to be the prime cytotoxic agent; rather there is strong evidence both *in vitro* and *in vivo* that the most toxic Aβ aggregates are small, soluble species that precede, but may also accompany, the appearance of mature fibrils (5).

We have generated a model system in which Aβ peptides are secreted from neurons in the brain of *Drosophila melanogaster* (6). The consequent phenotypes correlate well with the propensity of a range of Aβ variants to form soluble aggregates (7). Using this system, we performed an unbiased genetic modifier screen that highlighted the importance of iron metabolism as a cofactor in mediating the Aβ toxicity (8). Indeed, we and others have shown that both genetic and pharmacological manipulation of iron metabolism in the fly (8) and mouse (9) brain can modify Aβ toxicity. Notably, we found that overexpression of the heavy chain of the iron-binding protein ferritin affords a complete rescue of the locomotor deficits that result from Aβ expression (8). Iron accumulates in the brain with age (10, 11) and may have a role in the oxidative damage that is observed in AD (12–15), possibly by catalyzing the Fenton conversion of hydrogen peroxide to the highly toxic hydroxyl radical (8). Accordingly, we have shown that ferritin heavy chain can reduce oxidative damage in our model system; remarkably, ferritin is able to exert these beneficial effects despite a concomitant increase, sometimes more than 2-fold, in the accumulation of Aβ in the brains of flies (8). However, the role of iron in the aggregation of Aβ has been questioned because of the biophysical evidence that there is no high affinity interaction between the two (16). In this work, we employ fly, cell culture, and *in vitro* model systems to investigate how iron chelation renders Aβ aggregates non-toxic.

EXPERIMENTAL PROCEDURES

Drosophila Lines—D. melanogaster were cultured at 25 °C and grown on standard fly food containing 1% w/v agar, 8% w/v glucose, 8% w/v maize, 1.5% w/v yeast, 0.25% w/v Nipa-

* This work was supported by grants from the MRC (UK), Engineering and Physical Sciences Research Council (EPSRC) (UK), and Diabetes UK.

[S] The on-line version of this article (available at http://www.jbc.org) contains supplemental Fig. S1 and Materials and Methods.

[1] A Royal Society Dorothy Hodgkin Fellow.

[2] An Alzheimer's Research Trust Senior Research Fellow. To whom correspondence should be addressed: University of Cambridge, Dept. of Genetics, Downing St., Cambridge CB2 3EH, UK. E-mail: dcc26@cam.ac.uk.

[3] The abbreviations used are: AD, Alzheimer disease; Aβ, amyloid β; FerLCH, ferritin light chain; FerHCH, ferritin heavy chain; UAS, upstream activating sequence; h.e., hatching efficiency.

gin. UAS ferritin light chain (FerLCH) RNAi (CG1469) and UAS ferritin heavy chain (FerHCH) RNAi (CG2216) lines were obtained from the Vienna *Drosophila* RNAi Center. Flies carrying Aβ transgenes UAS-$A\beta_{1-40}$ (*Alz40.1*), UAS-$A\beta_{1-42}$ (*Alz42.3*), or UAS-*Arctic* $A\beta_{1-42}$ (*AlzArc1*) have been described previously (6).

Hatching Assays—Fly crosses were constructed to study the interaction between Aβ and ferritin RNAi. Offspring from the crosses inherited chromosomes carrying: i) *UAS-RNAi* constructs against *FerHCH* or *FerLCH* or control genetic background; ii) UAS-$A\beta_{40}$, UAS-$A\beta_{42}$, or UAS-Arctic$A\beta_{42}$ or control; and iii) *X,elav^{c155}-gal4* or *Y*. All the offspring from these crosses were counted ($n > 300$ flies for each combination of RNAi with Aβ transgene), and the hatching efficiency (h.e.) for each genotype was calculated, allowing for the genetic backgrounds of both the RNAi and the Aβ transgenes; it was assumed that genetic interactions were identical in male and female flies.

Treatment of Flies with the Iron Chelator YM-F24—YM-F24 was dissolved in dimethyl sulfoxide (the vehicle) and added to standard fly food at a maximum ratio of 0.2% v/v to achieve the 1000 μM condition. Developing and adult flies were cultured on tubes containing the appropriate concentration of compound throughout their life. Longevity assays were performed on 10 tubes of 10 flies for each condition as described previously (8).

Preparation of the $A\beta_{1-42}$ Peptide—$A\beta_{1-42}$ (H-1368 Bachem) peptide was dissolved in trifluoroacetic acid, sonicated, and lyophilized overnight. The peptides were then resuspended with gentle agitation in hexafluoroisopropyl alcohol to a concentration of 1 mg/ml for 30 min at 4 °C before aliquoting in the cold. The samples were dried under vacuum in a rotary evaporator for 3 h at room temperature and stored at −80 °C. Quantitative amino acid analysis was performed to measure the concentration and purity of the peptide (17).

Thioflavin T Assay of Amyloid Formation—Fluorescence assays were carried out using FLUOstar Optima plate reader with a 440-nm excitation filter and a 480-nm emission filter at 37 °C. Reactions were performed in black plastic, flat-bottomed 96-well Corning plates in a total volume of 100 μl. Each reaction mixture contained 20 μM thioflavin T, 5 μM $A\beta_{1-42}$ (Bachem), and a range of $FeCl_3$ concentrations (0–1000 μM) in modified Krebs-Henseleit buffer (123 mM NaCl, 4.8 mM KCl, 1.2 mM $MgSO_4$, 1.4 mM $CaCl_2$, 11.0 mM glucose, and 100 mM PIPES, pH 7.4). The plate was shaken for 5 s before each reading.

Aggregates to be used as seeds for further amyloid formation were generated by incubating $A\beta_{1-42}$ at 15 μM, with or without 1 mM iron, in Krebs-Henseleit buffer for 2 h at 37 °C. The aggregates were disrupted by sonication for 8 min and centrifuged at 18,000 × *g* for 10 min. The top 90% of supernatant was discarded, and the pellet was resuspended in the bottom 10% of the supernatant. 20 μl of this solution was used to seed each 100-μl aggregation reaction.

X-ray Fiber Diffraction—Freshly prepared $A\beta_{1-42}$ was dissolved at a concentration of 1 mM in ultrapure water ± 10 mM $FeCl_3$ and allowed to aggregate without agitation at 37 °C for 48 h. Droplets containing the fibrils were suspended between wax-coated glass rods and maintained in a sealed environment. During this desiccating treatment, the Aβ fibrils became aligned with the axis of the opposing glass rods. The dried bridging material was broken in half and placed in an x-ray beam with monitoring of the resulting diffraction pattern (18).

Transmission Electron Microscopy—4-μl aliquots of the $A\beta_{1-42}$ fibril suspension used for x-ray fiber diffraction studies were incubated on a copper mesh grid (size 400, S162-4 Formvar, Agar Scientific) for 1 min. The grids were then washed with 4 μl of water for 1 min before being stained twice in 4 μl of 2% w/v uranyl acetate in water.

Circular Dichroism Spectroscopy—$A\beta_{1-42}$ was dissolved at a concentration of 1 mM in ultrapure water ± 10 mM $FeCl_3$ in 5-μl aliquots and allowed to aggregate without agitation at 37 °C. At various time points, an aliquot was diluted 1:40 into ultrapure water, and the circular dichroism (CD) spectrum was measured in a quartz cuvette (path length 1 mm) using a JASCO J-810 spectrometer.

Tissue Culture—The human neuroblastoma cell line SH-SY5Y (94030304, Sigma) was cultured in Dulbecco's modified Eagle's medium/nutrient mixture F-12 Ham (Sigma D8437) supplemented with 20% v/v fetal bovine serum (F7524 Sigma), 100 units/liter penicillin, 100 mg/liter streptomycin (P4333 Sigma), 100 mg/liter kanamycin (K0129 Sigma). Cells were split 1:5 to 1:10 twice per week and incubated at 37 °C, 6% v/v $C0_2$. The cells were cultured for a maximum of 20 passages.

Cell Toxicity Assay—Cells were seeded overnight in normal culturing medium at 50,000 cells/well in a 96-well, sterile, Corning plate and washed twice the following morning with PBS. $A\beta_{1-42}$ fibrils were pelleted by ultracentrifugation (265,000 × *g* for 74 min at 25 °C in a TLA 100.3 rotor, Beckman Coulter) and diluted in Neurobasal (72349, Sigma) mixture containing the manufacturer's recommended concentration of glutamine (35050, Sigma) and N2 supplement (77502, Sigma). Cell viability was measured 18 h after incubation with $A\beta_{1-42}$ using a live/dead assay kit (L3224, Invitrogen) according to the manufacturer's instructions. Student's *t* test (two-tailed, paired) was used for testing significance between experimental conditions.

RESULTS

The Iron-specific Metal Chelator YM-F24 Prolongs the Life of Flies Expressing Aggregation-prone Aβ Peptides—Previous work has shown that treatment with the broad spectrum metal chelating agent, clioquinol, prolongs the life of flies expressing the most aggregation-prone isoforms of Aβ ($A\beta_{1-42}$ and Arctic $A\beta_{1-42}$) (8). Here we have tested whether the highly selective iron chelator YM-F24 (Fig. 1*a*) is able to rescue Aβ in a similar manner (Fig. 1*b*). Developing and then adult flies were cultured on food containing 40, 200, or 1000 μM YM-F24, and their longevity was compared with identical flies reared on food containing vehicle alone. Log-rank analysis revealed that YM-F24 had no significant effect on the survival of control (*circles*) or $A\beta_{1-40}$ (*crosses*) flies at any of the concentrations tested. In contrast, 1000 μM YM-F24 was able to significantly increase the survival of flies expressing $A\beta_{1-42}$

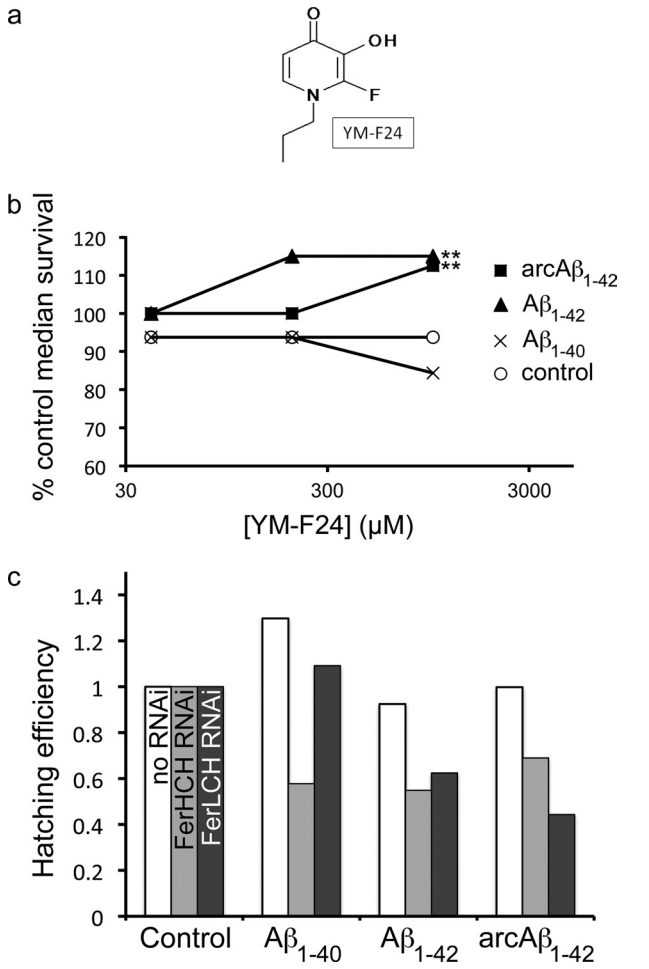

FIGURE 1. **Pharmacological and genetic manipulation of iron in the brain modifies the toxicity of Aβ.** *a*, the molecular structure of YM-F24. *b*, control flies (*circles*) or flies expressing $A\beta_{1-40}$ (*crosses*), $A\beta_{1-42}$ (*triangles*), or Arctic $A\beta_{1-42}$ (*arcAβ_{1-42}*, *squares*) were treated with 40, 200, or 1000 μM YM-F24 or vehicle alone, and the percentage of increase in median survival was plotted. Log-rank survival analysis indicated that 1000 μM YM-F24 was able to significantly increase the longevity of flies expressing $A\beta_{1-42}$ and Arctic $A\beta_{1-42}$ ($n = 100$ flies for each test; **, $= p < 0.01$). No other differences were significant. *c*, the degree of synthetic lethality caused by Aβ and ferritin RNAi co-expression was determined by measuring hatching efficiency. For flies expressing each Aβ variant ($A\beta_{1-40}$, $A\beta_{1-42}$, Arctic $A\beta_{1-42}$, and controls), genetic crosses were set up, and all four classes of offspring were counted ($\pm A\beta \times \pm$ RNAi). The hatching efficiency for flies expressing Aβ was expressed as the -fold change from the expected values as determined by the control crosses. Co-expression of FerHCH RNAi (*light gray bars*) with all three Aβ peptides reduced hatching efficiency; however, FerLCH RNAi (*dark gray bars*) only reduced hatching efficiency for the more aggregation-prone $A\beta_{1-42}$ and Arctic $A\beta_{1-42}$ peptides. Control flies not expressing RNAi constructs (*white bars*) did not show a reduction in hatching efficiency. χ^2 testing of the differences between observed and predicted numbers of hatching flies (total = 626) for all conditions was significant ($p = 5 \times 10^{-9}$). A total of 3468 flies were counted to calculate the expected hatching frequencies. The data are representative of two independent experiments.

(*triangles*, 15% increase) and Arctic $A\beta_{1-42}$ (*squares*, 12.5% increase).

RNAi Knockdown of the Iron-binding Protein Ferritin Enhances Aβ Lethality in Our Drosophila Model System—Increasing the iron binding capacity of the brain by overexpressing ferritin subunits has also been shown to protect against Aβ toxicity (8). In this light, we tested whether the converse intervention, that is, the RNAi-mediated knockdown of the same genes, might be detrimental (Fig. 1*c*). Remarkably, we found that ferritin RNAi co-expression with Aβ in the brain resulted in synthetic lethality that was particularly severe when combined with Arctic $A\beta_{1-42}$. We quantified this effect by measuring the hatching efficiency (h.e.) for each of the fly genotypes. When we controlled for the effect of RNAi expression in control flies (Fig. 1*c*, *Control*) that do not express Aβ, we found that flies expressing $A\beta_{1-40}$ were insensitive to the co-expression of FerLCH RNAi (*dark gray bars*, h.e. = 109% *versus* 130% for controls (*white bars*)); however, in the same flies, FerHCH RNAi was clearly toxic (*light gray bars*, h.e. = 57%). For the more aggregation-prone isoforms of Aβ, namely $A\beta_{1-42}$ and Arctic $A\beta_{1-42}$, the hatching efficiency was similarly reduced for both FerHCH and FerLCH RNAi constructs (h.e. = 44–69% for Aβ flies, *gray bars versus* 92–100% for controls (*white bars*)). χ^2 testing of the differences between observed and predicted numbers of hatched flies indicated a highly likely interaction between Aβ expression and ferritin RNAi ($p = 5 \times 10^{-9}$). These data indicate that endogenous ferritin is important in protecting the fly against Aβ toxicity. The goal of the study presented here was to determine whether unchelated iron may promote toxicity by modulating the Aβ aggregation pathway (19).

Iron Causes $A\beta_{1-42}$ to Form Less Ordered Aggregates in Vitro—The morphology of Aβ assemblies was determined, in the presence and absence of iron, using transmission electron microscopy. When it was incubated without iron, we found that $A\beta_{1-42}$ formed typical, straight, unbranched amyloid fibrils (Fig. 2, *a* and *b*, *arrows*). However, in the presence of a 10-fold molar excess of iron(III), the fibrils were shorter (Fig. 2, *c* and *d*). We quantified the differences in morphology by tracing representative fibrils for the two conditions (Fig. 2*e*). When we aligned the fibrils and measured the length of the bounding rectangle, we found that fibrils generated in the presence of iron were significantly shorter than those generated in the absence of iron (Fig. 2*f*, 160 *versus* 570 nm, *bars* = S.E., $p = 2 \times 10^{-9}$). This morphological change in the amyloid fibrils with iron is compatible with them adopting a less ordered structure that may in turn increase the specific toxicity of the peptide.

Studies of these fibrils using x-ray fiber diffraction confirmed the presence of typical cross-β structure (20) both in the absence (Fig. 3*a*) and in the presence (Fig. 3*b*) of iron. The characteristic features of amyloid fibrils are the 4.6 Å reflections on the meridian (Fig. 3*a*, ***1***, and 3*b*, ***5***) and the 9.6 Å reflections on the equator (Fig. 3*a*, *2*, and 3*b*, ***6***). The reflections are more intense in the absence of iron; the good alignment of the fibrils in the absence of iron allowed the visualization of previously unreported reflections for Aβ fibrils at 24.5 Å (Fig. 3*a*, ***3***) and 14.4 Å (Fig. 3*a*, ***4***). The reduced quality of the diffraction pattern obtained in the presence of iron most likely reflects the poor alignment of the fibrils due to their short and curved nature.

The Progression to β-Structure Is Impeded by the Presence of Iron—Circular dichroism spectroscopy was used to monitor the development of secondary structure when Aβ was incubated in the presence and absence of iron. In the absence of iron, 10 μM $A\beta_{1-42}$ progressed to a predominantly β-sheet

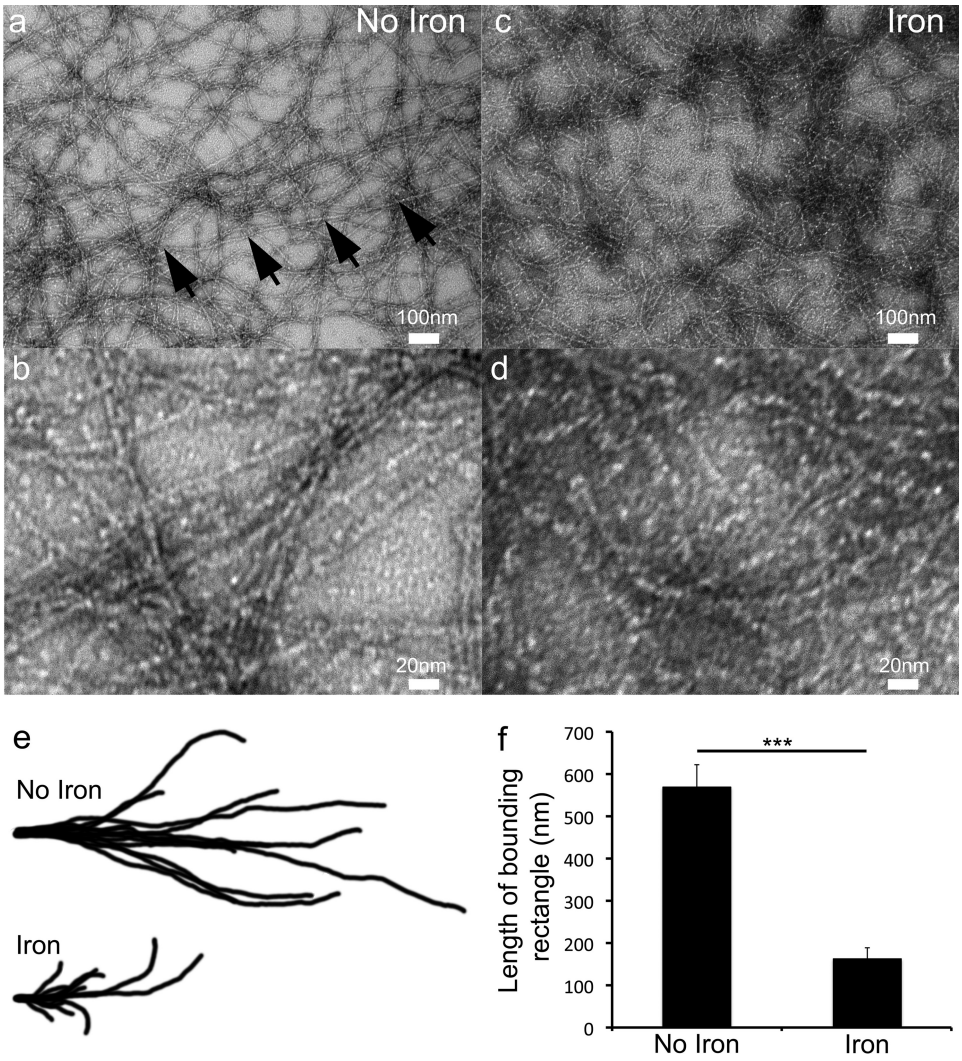

FIGURE 2. **Iron affects the morphology of Aβ_{1-42} fibrils.** When visualized using transmission electron microscopy, Aβ_{1-42} fibrils generated in the absence of iron (*a* and *b*, *No Iron*, *arrows*) are longer and straighter than fibrils formed in the presence of a 10-fold molar excess of iron(III) (*c* and *d*, *Iron*). *Scale bars* represent 100 nm in *a* and *c* and 20 nm in *b* and *d*. Typical fibrils are indicated by *arrows*. *e*, 13 representative fibrils formed in the absence and presence of iron were traced and aligned such that their initial tangent was horizontal (33). *f*, the horizontal length of the bounding rectangle for each fibril (a combined measure of length and straightness) was greater in the absence of iron than in the presence (mean lengths ± S.E.). The paired two-tailed Student's *t* test was used for statistical analysis (***, $p = 2 \times 10^{-5}$).

profile within the first 15 min (Fig. 4*a*, *white triangles*). However, in the presence of iron, this structural progression was impeded such that the peptide remains in intermediate conformations for longer (Fig. 4*b*, 15 min (*open triangles*) and 30 min (*open rectangles*)). As proteins gain β-sheet structure, there is usually a negative change in molar ellipticity at 216 nm. When the signal at 216 nm was plotted against time (Fig. 4*c*), the delay in the transition to a β-rich structure in the presence of iron (*dashes*), as compared with peptide alone (*solid*), was readily apparent. These data show that Aβ takes longer to progress to its final structure in the presence of iron and that this kinetic stabilization of intermediate species may explain the role of iron as a modulator of toxicity.

The Modulation of Aβ Aggregation by Iron Abolishes Thioflavin T Fluorescence—Fluorescent dyes such as thioflavin T are widely used to detect the presence of amyloid aggregates in solutions (21, 22). We confirm that, as expected, the aggregation of Aβ, in the absence of iron(III) (Fig. 5*a*, *gray dots*), is accompanied by a robust thioflavin T fluorescence signal. However, for iron(III) concentrations exceeding 16 μM (Fig. 5*a*, *black solid line*), we found that the consequent fluorescence signal was reduced. This signal was abolished by the addition of 250 μM iron(III) or higher (Fig. 5*a*, *black dashes* and *dots*). The abolition of the thioflavin T fluorescence occurred despite the presence of amyloid fibrils as determined by transmission electron microscopy (Fig. 2, *c* and *d*).

To control for the possibility that the loss of thioflavin T signal seen in Fig. 5*a* was caused by competition between iron and dye for access to the aggregates (23), we undertook the experiment shown in Fig. 5*b*. Two standard aggregation reactions were set up, with thioflavin T present from the start (*black lines*), either in the presence (*solid*) or in the absence (*dots*) of 1 mM $FeCl_3$. Two additional aggregation reactions (*gray lines*) were constructed in the same way except that thioflavin T was added either at time A (*dots*) or at time B (*solid*). Conversely, iron was added, to a final concentration of

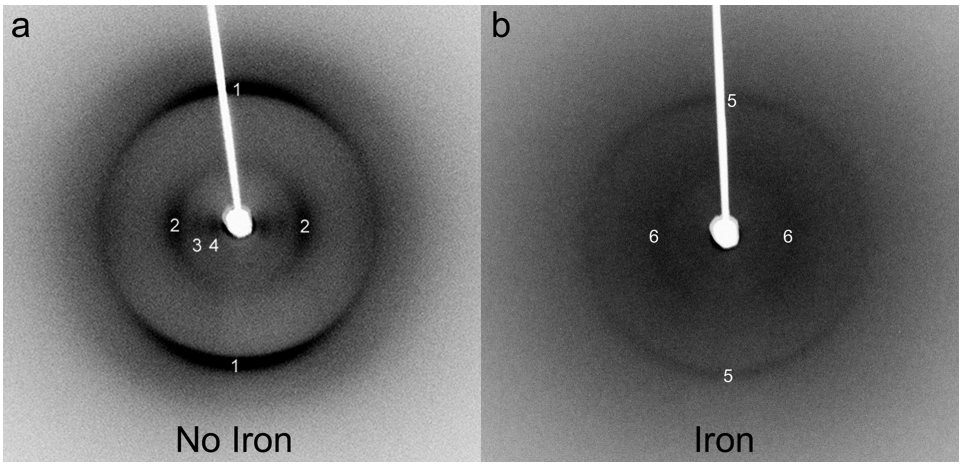

FIGURE 3. **Iron modulates the degree of order in $A\beta_{1-42}$ fibrils as determined by x-ray fiber diffraction.** *a*, x-ray fiber diffraction patterns from $A\beta_{1-42}$ fibrils formed in the absence of iron (*No Iron*) yield high definition reflections that are consistent with a classical cross-β structure: specifically, 4.66 Å reflections at the meridian (***1***) and 9.66 Å reflections at the equator (***2***). Previously unreported reflections were also seen at 14.4 Å (***3***) and 24.5 Å (***4***). *b*, $A\beta_{1-42}$ fibrils formed in the presence of a 10-fold molar excess of iron(III) (*Iron*) exhibit poor alignment within the fiber, and so the quality of the diffraction pattern was diminished. Despite this, the signature reflections at 4.6 Å (***5***) and 9 Å (***6***) indicate that a component of cross-β structure was retained. The data are representative of two independent experiments.

1 mM at times A (*solid*) and B (*dots*). The convergence of both *gray traces* at time B demonstrated that there was no competition between iron and thioflavin T for access to preformed Aβ fibrils.

To test whether the fibrils formed in the presence and absence of iron might constitute different strains of amyloid, we investigated their respective seeding properties. Fibrils of $A\beta_{1-42}$ were generated in the absence or presence of iron by incubation in Krebs-Henseleit buffer overnight at room temperature. The fibrils were disrupted by sonication and spiked into a fresh aggregation reaction. As compared with unseeded $A\beta_{1-42}$ (Fig. 5*c*, *black bar*), the iron-free thioflavin T kinetics were unchanged upon the addition of plus-iron seeds (*white bar*). In contrast, no-iron seeds added in the same way were able to significantly reduce the thioflavin T lag time (*gray bar*, $p < 0.01$).

The Presence of Iron during the Aggregation of $A\beta_{1-42}$ Favors the Generation of Toxic Species—A live/dead cell viability assay was used to investigate the iron-mediated modulation of $A\beta_{1-42}$ toxicity in cultures of human neuroblastoma (SH-SY5Y) cells. Our initial experiments showed that $FeCl_3$ concentrations up to four times higher than those used in subsequent experiments were not cytotoxic (Fig. 6*a*). $A\beta_{1-42}$ aggregates are cytotoxic (24, 25), and so we performed serial dilutions of the peptide to determine the concentration dependence of this effect (Fig. 6*b*). In our system, 10 μM Aβ represented a threshold above which, in the absence of iron, toxicity increased sharply, and so we chose this concentration for subsequent cell culture experiments. We then tested for an interaction between iron and Aβ in generating cytotoxicity. As shown in Fig. 6*c*, 10 μM $A\beta_{1-42}$ (*first bar*) was no more toxic than culture medium alone (*fourth bar*). Similarly, when $A\beta_{1-42}$ was allowed to aggregate in the absence of iron (with iron being added when aggregation was complete), there was again no significant toxicity (*second bar*). Remarkably, the presence of iron during the process of Aβ aggregation reduced the live/dead ratio by over 20% (*third bar*, $p < 0.04$). Flow cytometric measurement of surface-expressed annexin V (see supplemental Materials and Methods) indicated that the mechanism of cell death is likely to be apoptotic. Specifically, 56% of cells treated with Aβ aggregated in the presence of iron were annexin V-positive. The corresponding proportion was only 19% for cells treated with Aβ aggregates that had been formed in the absence of iron and subsequently spiked with iron (supplemental Fig. S1).

DISCUSSION

Metal ions are strongly implicated as cofactors in the pathogenesis of AD. Indeed, many investigators have shown that copper, zinc, and iron can exacerbate the oxidative damage that accompanies Aβ peptide aggregation (26–28). Furthermore, iron and other metals are present in high concentrations in amyloid plaques in the brains of individuals with AD (29). The importance of iron was highlighted by our genetic screen in a *Drosophila* model system that faithfully reports the toxicity of soluble aggregates of Aβ (7, 17). In that study, we generated fly lines that exhibited altered sensitivity to Aβ toxicity, and remarkably, the most powerful phenotypic rescue was seen in flies where subunits of the iron-binding protein ferritin were co-overexpressed with Aβ. We showed that this rescue was accompanied by a reduction in the oxidative damage in the brain, and furthermore, our genetic dissection pointed to the generation of the hydroxyl radical, by the iron-catalyzed Fenton reaction, as the most important pathological step (8). However, our previous study left unexplained the observation that flies expressing both the heavy and the light chains of ferritin showed phenotypic rescues despite accumulating more Aβ in their brains. Under such conditions, the Aβ deposits are more stable and less toxic. These findings support a dual role for iron in generating toxicity, firstly by acting as a cofactor in the generation of reactive oxygen species via the Fenton reaction, a mechanism that

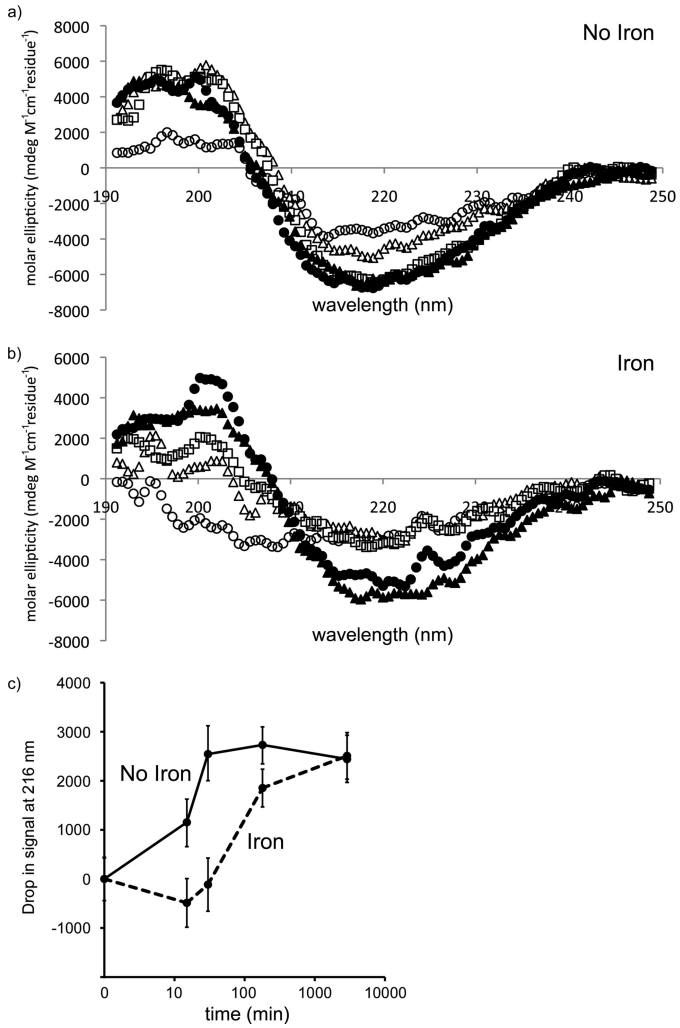

FIGURE 4. **Iron impedes the structural progression of Aβ_{1-42} from unstructured monomer to β-rich fibril.** *a*, in the absence of iron (*No Iron*), Aβ_{1-42} rapidly progresses from an unstructured to a β-rich conformation. At $t = 0$ min (*open circles*) and $t = 15$ min (*open triangles*), the transition to β-structure is incomplete, but by $t = 30$ min (*open squares*), the reaction has reached its end point, and the spectrum is unchanged at $t = 180$ min (*filled circles*) and $t = 2880$ min (*filled triangles*). *mdeg*, millidegrees. *b*, in the presence of a 10-fold molar excess of iron(III) (*Iron*) the structural progression is impeded such that at $t = 0$, 15, and 30 min (*open circles*, *triangles*, and *squares*), the reactions exhibit intermediate spectra. By $t = 180$ and 2880 min (*filled circles* and *triangles*), the final β-rich spectrum has been achieved. *c*, the change in molar ellipticity at 216 nm was plotted against time for Aβ_{1-42} incubated in the presence (*dashes*) or absence (*solid*) of 1 mM $FeCl_3$. Three independent experiments were performed, and the values plotted represent the mean (±S.E.).

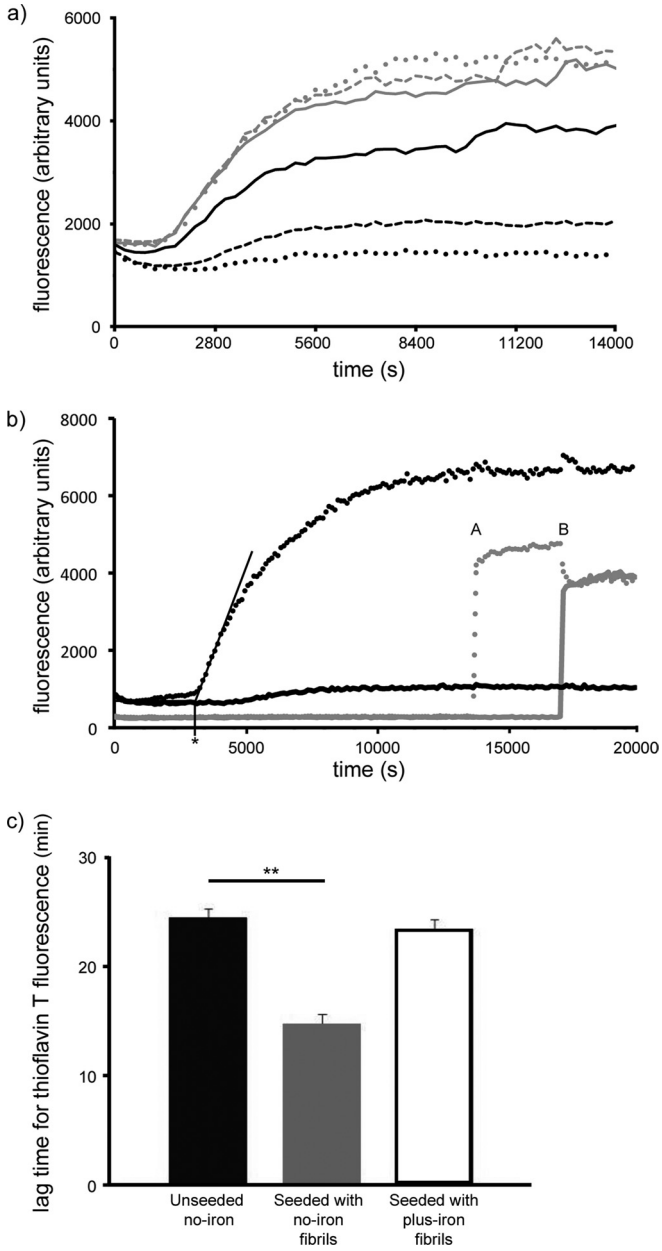

FIGURE 5. **Iron abolishes the thioflavin T fluorescence signal of Aβ aggregation.** *a*, there was no effect of 0 μM (*gray dots*), 5 μM (*gray dashes*), and 16 μM (*gray line*) iron(III) on the thioflavin T fluorescence signal during Aβ_{1-42} aggregation. However, the signal was reduced (*black line*, 63 μM) and then abolished (*black dashes* = 250 μM and *black dots* = 1000 μM) at higher concentrations of iron. *b*, with thioflavin T present throughout the reaction, the addition of 1 mM $FeCl_3$ (*solid*) prevented the increase in fluorescence as compared with Aβ alone (*dots*). When no thioflavin T was added until after Aβ_{1-42} aggregation (*gray traces*), the final fluorescence signal was unchanged irrespective of whether iron was added first (*solid*, *transition A*) followed by thioflavin T (*solid*, *transition B*) or vice versa (*dots*, *A* and *B*). An example of the lag time calculation for the *black dotted trace* is shown by the *asterisk*. *c*, the lag time for the iron-free thioflavin T fluorescence signal was determined for unseeded Aβ_{1-42} aggregation (*black*, *Unseeded no-iron*), for Aβ_{1-42} seeded with fibrils that had been grown in the absence of iron (*gray*, *Seeded with no-iron fibrils*), and for Aβ_{1-42} seeded with fibrils that had been grown in the presence of iron (*white*, *Seeded with plus-iron fibrils*). Only fibrils that formed in the absence of iron were able to seed the iron-free fibrillization of Aβ_{1-42}. The lag time was calculated by extending the tangent at the point of inflection of the fluorescence trace and determining the intersection with the minimum fluorescence signal measured (see *asterisk* in *panel b*). Three independent experiments were performed, and the values plotted represent the mean (±S.E.). The paired two-tailed Student's *t* test was used for statistical analysis (**, $p < 0.01$).

requires the presence of Fe(II) ion. In this regard, we previously found that overexpression of FerHCH was most effective at suppressing toxicity presumably because, in addition to the chelating role it shares with FerLCH, the heavy chain subunit is also able to oxidize Fe(II) to the less redox-active Fe(III). The second role for iron is likely to be as a modulator of Aβ aggregation. The goals of the current study were to confirm the interaction between iron binding and Aβ toxicity in our *in vivo* model and then to look at the effects that iron had on aggregation and consequent toxicity.

Our first experiments confirmed the importance of iron metabolism in Aβ toxicity by treating flies with the iron-se-

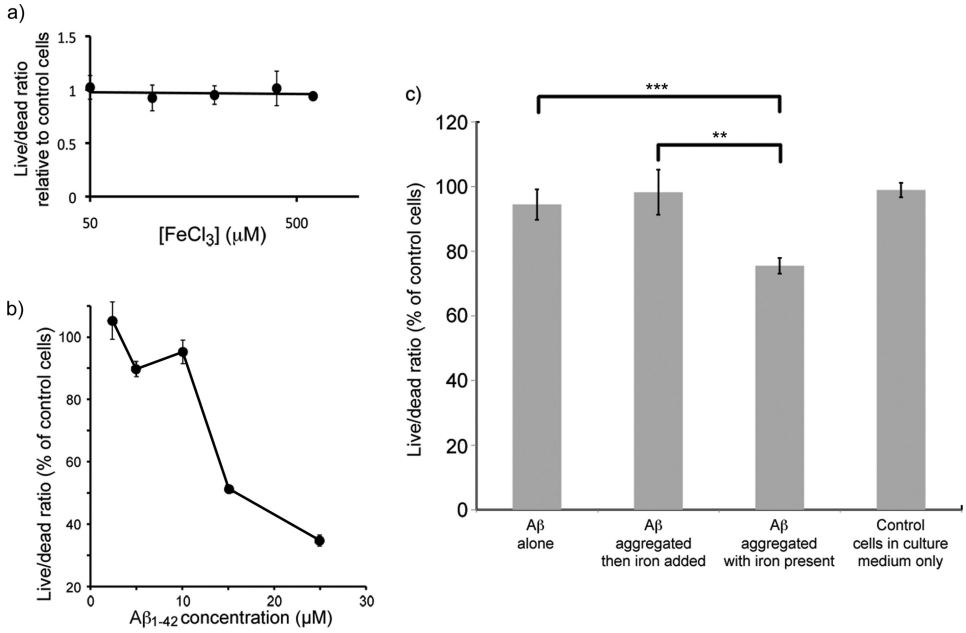

FIGURE 6. **The presence of iron during the aggregation of $A\beta_{1-42}$ increases the *in vitro* toxicity of the resulting aggregates.** *a*, the addition of $FeCl_3$ (which will rapidly form iron(III) hydroxide) at increasing concentrations to the culture medium of SH-SY5Y cells did not result in appreciable toxicity even when concentrations were 6-fold higher than used in subsequent experiments. *b*, serial dilutions of $A\beta_{1-42}$ demonstrated that above 10 μM, there was a rapid concentration-related increase in cytotoxicity. For this reason, 10 μM $A\beta_{1-42}$ was used in the subsequent experiments. *c*, as compared with SH-SY5Y cells grown in culture medium alone (*Control cells in culture medium only*), there was no extra toxicity observed in the presence of freshly prepared 10 μM $A\beta_{1-42}$ (*Aβ alone*), with 10 μM $A\beta_{1-42}$ that had been aggregated in the absence of iron and then spiked with iron(III) (*Aβ aggregated then iron added*), or with iron alone (*panel a*). In contrast, 10 μM $A\beta_{1-42}$ that had been aggregated in the presence of iron(III) (*Aβ aggregated with iron present*) caused a greater than 20% decrease in the live/dead ratio (***, $p = 0.01$ *versus* Aβ alone and **, $p = 0.04$ *versus* Aβ then iron). Three biological replicates were performed with $n = 8$ for each condition for each replicate. The values plotted represent the mean (±S.E.). The paired two-tailed Student's *t* test was used for statistical analysis.

lective chelating agent YM-F24. Previous data showing that the broad spectrum metal chelator clioquinol could rescue Aβ toxicity did not permit a dissection of the relative significance of copper, zinc, or iron. The finding that YM-F24 can significantly prolong the lifespan of flies expressing the aggregation-prone $A\beta_{1-42}$ and Arctic $A\beta_{1-42}$ peptides indicates that iron does indeed have an important role in mediating toxicity. We also probed the endogenous iron binding capacity of the fly by observing the effect of RNAi knockdown of endogenous *Drosophila* ferritin. We found the interaction between Aβ expression and ferritin RNAi to be remarkably strong, with high levels of synthetic lethality, particularly in flies expressing $A\beta_{1-42}$ and Arctic $A\beta_{1-42}$ in their brains. For this reason, we could not perform longevity assays, and instead, we quantified the developmental lethality. When we controlled for the lethality associated with ferritin RNAi in control flies not expressing Aβ, we found that the interaction between the two was particularly apparent for $A\beta_{1-42}$ and Arctic $A\beta_{1-42}$. For both these peptides, the co-expression of FerHCH and FerLCH RNAi constructs increased the lethality (h.e. = 44–69% for Aβ flies with the RNAi *versus* 92–100% for controls with the RNAi). For flies expressing the normally non-toxic $A\beta_{1-40}$, we found that co-expression of FerHCH, but not FerLCH, RNAi constructs caused a large reduction in hatching efficiency (h.e. = 57% for $A\beta_{1-40}$ *versus* 109% for controls). It is interesting to note that although FerLCH RNAi is increasingly lethal in combination with Aβ isoforms of increasing aggregation propensity, the same is not true for FerHCH RNAi. We speculate that this may reflect the differing biological properties of the ferritin subunits, in particular the presence of ferroxidase activity in the heavy chain that is not present in the light chain. However, the precise reason for these differences has not been established.

The protection afforded by the iron-selective chelator YM-F24 and the link between ferritin RNAi and reduced hatching efficiency in the presence of Aβ confirmed iron as a cofactor in the generation of Aβ toxicity. This is concordant with our previous finding that in the presence of ferritin overexpression, Aβ can accumulate to high levels and yet fails to induce toxicity. To understand how the specific toxicity of the Aβ aggregates might be reduced in the absence of iron, we studied the effect of iron on the aggregation properties of $A\beta_{1-42}$ using a number of biophysical techniques. Specifically, x-ray fiber diffraction demonstrated that the presence of iron during the aggregation of $A\beta_{1-42}$ resulted in fibrils that were less ordered than control reactions performed in the absence of iron (Fig. 2). The regular and elongated morphology of the iron-free fibrils would predictably favor their ordered alignment within the x-ray diffraction sample and probably accounts for the high definition images that were obtained in such conditions (Fig. 3*a*). The principal x-ray diffraction findings were characteristic cross-β reflections at 4.6 Å on the meridian and at 9.6 Å on the equator. There were also novel reflections present indicating longer range repeats in fibril structure of 14.4 and 24.5 Å. The fibrils formed in the presence of iron also showed characteristic 4.6 and 9.6 Å reflections; however, the quality of the images was poor, most likely because of

irregular fibril alignment, although increased disorder within the fibrils themselves is also possible. It is notable that there are no intense iron spots in Fig. 3*b*, indicating that iron is not stably bound to the peptides in the fibrils (30).

Thus iron can alter the structure of Aβ amyloid by favoring the generation of less ordered fibrils. To investigate the kinetics of this effect, we used CD spectroscopy to determine how iron affected the generation of secondary structure. Both in the presence and in the absence of iron, there was a progressive increase in β-sheet structure with time (Fig. 4, *a versus b*, and 4*c*); however, iron was seen to impede this structural progression. Iron was able to delay the formation of a mature amyloid population by increasing the lifespan of smaller, soluble species that are thought to be most toxic *in vivo*. The kinetics of aggregation were also studied using thioflavin T fluorescence in the presence of increasing concentrations of iron. In these experiments, there is a remarkable reduction in the fluorescence signal as the iron concentration is increased (Fig. 5*a*) despite the formation of amyloid fibrils as determined by electron microscopy. This loss of signal is not due to competition between iron and thioflavin T for access to the fibrils because fibrils that were formed in the absence of iron but then spiked with iron generated a normal fluorescence signal when thioflavin T was subsequently added (Fig. 5*b*). Remarkably, we were able to show that there is a strain-like difference between fibrils generated in the presence or absence of iron. Specifically, we have demonstrated that fibrils generated in the presence of iron are not able to seed the generation of Aβ amyloid when iron is no longer present.

These data strongly suggest that although the aggregates formed by Aβ in the presence and absence of iron share some cross-β structure, they differ in two important ways. Firstly, the final structure in the presence of iron is distinctly less ordered and does not interact with thioflavin T. Secondly, the kinetics of Aβ aggregation are slowed, and intermediate conformers are stabilized.

Next we assessed whether these differences in aggregate conformation were mirrored by differential cytotoxicity. We found that neither 10 μM freshly prepared Aβ nor iron alone (in the form of the hydroxide) was toxic when added to SH-SY5Y cells. Likewise Aβ did not acquire toxicity when it was allowed to aggregate in the absence of iron and then spiked with iron. In contrast, the presence of iron during the Aβ aggregation reaction caused robust toxicity, resulting in a greater than 20% reduction in the live/dead ratio as compared with the other conditions (Fig. 6*c*). Measurement of the surface expression of annexin V using flow cytometry showed that this marker of apoptosis is greatly increased when iron is present during the Aβ aggregation reaction as compared with control reactions that were spiked after aggregation (supplemental Fig. S1).

These observations help us to understand how iron can have profound effects on the toxicity of the Aβ peptide despite the absence of any observable high affinity interaction *in vivo* (30). Although recent *in vitro* studies have shown that iron can interact with soluble Aβ (31), we find that iron is not incorporated into amyloid, but rather it delays the formation of mature, well ordered, fibrillar aggregates. This iron-mediated stabilization of soluble intermediate Aβ species, probably by modifying the kinetics of aggregation through low affinity interactions, explains much, if not all, of the toxicity observed in our experimental models. These findings further justify the search for potent iron-chelating agents such as YM-F24 that may have therapeutic value in Alzheimer disease (32) by favoring the non-toxic deposition of Aβ.

REFERENCES

1. Yankner, B. A., and Lu, T. (2009) *J. Biol. Chem.* **284,** 4755–4759
2. Walsh, D. M., and Selkoe, D. J. (2007) *J. Neurochem.* **101,** 1172–1184
3. Nilsberth, C., Westlind-Danielsson, A., Eckman, C. B., Condron, M. M., Axelman, K., Forsell, C., Stenh, C., Luthman, J., Teplow, D. B., Younkin, S. G., Näslund, J., and Lannfelt, L. (2001) *Nat. Neurosci.* **4,** 887–893
4. Hardy, J. A., and Higgins, G. A. (1992) *Science* **256,** 184–185
5. Lambert, M. P., Barlow, A. K., Chromy, B. A., Edwards, C., Freed, R., Liosatos, M., Morgan, T. E., Rozovsky, I., Trommer, B., Viola, K. L., Wals, P., Zhang, C., Finch, C. E., Krafft, G. A., and Klein, W. L. (1998) *Proc. Natl. Acad. Sci. U.S.A.* **95,** 6448–6453
6. Crowther, D. C., Kinghorn, K. J., Miranda, E., Page, R., Curry, J. A., Duthie, F. A., Gubb, D. C., and Lomas, D. A. (2005) *Neuroscience* **132,** 123–135
7. Luheshi, L. M., Tartaglia, G. G., Brorsson, A. C., Pawar, A. P., Watson, I. E., Chiti, F., Vendruscolo, M., Lomas, D. A., Dobson, C. M., and Crowther, D. C. (2007) *PLoS. Biol.* **5,** e290
8. Rival, T., Page, R. M., Chandraratna, D. S., Sendall, T. J., Ryder, E., Liu, B., Lewis, H., Rosahl, T., Hider, R., Camargo, L. M., Shearman, M. S., Crowther, D. C., and Lomas, D. A. (2009) *Eur. J. Neurosci.* **29,** 1335–1347
9. Grossi, C., Francese, S., Casini, A., Rosi, M. C., Luccarini, I., Fiorentini, A., Gabbiani, C., Messori, L., Moneti, G., and Casamenti, F. (2009) *J. Alzheimers. Dis.* **17,** 423–440
10. Connor, J. R., Menzies, S. L., St Martin, S. M., and Mufson, E. J. (1990) *J. Neurosci. Res.* **27,** 595–611
11. Zecca, L., Stroppolo, A., Gatti, A., Tampellini, D., Toscani, M., Gallorini, M., Giaveri, G., Arosio, P., Santambrogio, P., Fariello, R. G., Karatekin, E., Kleinman, M. H., Turro, N., Hornykiewicz, O., and Zucca, F. A. (2004) *Proc. Natl. Acad. Sci. U.S.A.* **101,** 9843–9848
12. Nunomura, A., Perry, G., Aliev, G., Hirai, K., Takeda, A., Balraj, E. K., Jones, P. K., Ghanbari, H., Wataya, T., Shimohama, S., Chiba, S., Atwood, C. S., Petersen, R. B., and Smith, M. A. (2001) *J. Neuropathol. Exp. Neurol.* **60,** 759–767
13. Nunomura, A., Perry, G., Pappolla, M. A., Wade, R., Hirai, K., Chiba, S., and Smith, M. A. (1999) *J. Neurosci.* **19,** 1959–1964
14. Sayre, L. M., Zelasko, D. A., Harris, P. L., Perry, G., Salomon, R. G., and Smith, M. A. (1997) *J. Neurochem.* **68,** 2092–2097
15. Smith, M. A., Perry, G., Richey, P. L., Sayre, L. M., Anderson, V. E., Beal, M. F., and Kowall, N. (1996) *Nature* **382,** 120–121
16. Wan, L., Nie, G., Zhang, J., Luo, Y., Zhang, P., Zhang, Z., and Zhao, B. (2010) *Free Radic. Biol. Med.*, in press
17. Brorsson, A. C., Bolognesi, B., Tartaglia, G. G., Shammas, S. L., Favrin, G., Watson, I., Lomas, D. A., Chiti, F., Vendruscolo, M., Dobson, C. M., Crowther, D. C., and Luheshi, L. M. (2010) *Biophys. J.* **98,** 1677–1684
18. Makin, O. S., and Serpell, L. C. (2005) *Methods Mol. Biol.* **299,** 67–80
19. Selkoe, D. J. (2003) *Nature* **426,** 900–904
20. Sunde, M., Serpell, L. C., Bartlam, M., Fraser, P. E., Pepys, M. B., and Blake, C. C. (1997) *J. Mol. Biol.* **273,** 729–739
21. LeVine, H., 3rd (1999) *Methods Enzymol.* **309,** 274–284
22. Rogers, D. R. (1965) *Am. J. Clin. Pathol.* **44,** 59–61
23. Hudson, S. A., Ecroyd, H., Kee, T. W., and Carver, J. A. (2009) *FEBS J.* **276,** 5960–5972
24. Li, Y. P., Bushnell, A. F., Lee, C. M., Perlmutter, L. S., and Wong, S. K. (1996) *Brain Res.* **738,** 196–204

25. Huang, J., and May, J. M. (2006) *Brain Res.* **1097,** 52–58
26. Garzon-Rodriguez, W., Yatsimirsky, A. K., and Glabe, C. G. (1999) *Bioorg. Med. Chem. Lett.* **9,** 2243–2248
27. Huang, X., Moir, R. D., Tanzi, R. E., Bush, A. I., and Rogers, J. T. (2004) *Ann. N.Y. Acad. Sci.* **1012,** 153–163
28. Smith, D. G., Cappai, R., and Barnham, K. J. (2007) *Biochim. Biophys. Acta* **1768,** 1976–1990
29. Bush, A. I. (2003) *Trends Neurosci.* **26,** 207–214
30. Dong, J., Atwood, C. S., Anderson, V. E., Siedlak, S. L., Smith, M. A., Perry, G., and Carey, P. R. (2003) *Biochemistry* **42,** 2768–2773
31. Nair, N. G., Perry, G., Smith, M. A., and Reddy, V. P. (2010) *J. Alzheimers Dis.* **20,** 57–66
32. Molina-Holgado, F., Hider, R. C., Gaeta, A., Williams, R., and Francis, P. (2007) *Biometals* **20,** 639–654
33. Knowles, T. P., Fitzpatrick, A. W., Meehan, S., Mott, H. R., Vendruscolo, M., Dobson, C. M., and Welland, M. E. (2007) *Science* **318,** 1900–1903